

## SPIN-AXIS TILT ESTIMATION ALGORITHM WITH VALIDATION BY REAL DATA

Halil Ersin Soken,<sup>\*</sup> Jozef C. Van der Ha<sup>†</sup> and Shin-ichiro Sakai<sup>‡</sup>

The spin-axis tilt (SAT), which is also known as dynamic imbalance or coning error, is one of the dominant errors deteriorating the attitude determination accuracy of spinning spacecraft. It is experienced as the misalignment of the major principal axis of the spacecraft from the intended body spin axis. This paper evaluates a straightforward SAT estimation algorithm by means of real in-flight data. The algorithm is based on the Singular Value Decomposition (SVD) method and makes use of the attitude rates estimated by an attitude determination filter. The accuracy of the algorithm is investigated by using telemetry data gathered by the CONTOUR spacecraft in 2002. The results are compared with those obtained by an averaging method for the SAT determination. The SVD-based SAT estimation algorithm (SVD-SAT) provides robust estimation results without being significantly affected by sensor biases. This is in contrast with the averaging method, which is shown to be more sensitive to other errors.

### INTRODUCTION

The spin-axis tilt (SAT) is one of the most significant bias errors that deteriorate the estimation accuracy of the spin-axis orientation of spinning spacecraft<sup>1,2</sup>. The tilt is observed as the angular deviation between the actual spin axis (i.e., one of the principal axes) and the intended or designed spin axis (i.e., one of the designated body axes). This error is also known as coning error<sup>3,4</sup> or dynamic imbalance.

There are usually many reasons for experiencing SAT in a spinning spacecraft. Most commonly, the tilt may be caused by residual errors in the dynamical balancing during the assembly and integration; vibrations during the launch; and unmodeled in-flight variations of mass and inertias<sup>5</sup>. Changes in the mass distribution may be due to liquid propellants and/or flexible appendages. Moreover, the spin-axis tilt may vary over time and is not necessarily constant for all mission duration. Thermal dilation effects, propellant usage or sloshing, and outgassing may also cause changes in the tilt angle. In fact, any variation in the spacecraft dynamical behavior may be considered as an indication for a change in the SAT. Even though they are usually small in magnitude, such changes may even be experienced within one orbit period. As an example, Ref. 6

---

<sup>\*</sup> Aerospace Project Research Associate, Institute of Space and Astronautical Science (ISAS), Japan Aerospace Exploration Agency (JAXA), Yoshinodai 3-1-1 Chuo-ku, Sagami-hara 252-5210 Japan.

<sup>†</sup> Aerospace Engineering Consultant, Satellite Mission Design and Operations, 5808 Bell Creek Road, Deming, WA 98244, USA.

<sup>‡</sup> Associate Professor, Institute of Space and Astronautical Science (ISAS), Japan Aerospace Exploration Agency (JAXA), Yoshinodai 3-1-1 Chuo-ku, Sagami-hara 252-5210 Japan.

discusses how the spacecraft dynamics change in various cases including the perigee pass and eclipse for NASA's Van Allen Probes, a recent spinning spacecraft mission.

Effects of the SAT on the attitude determination accuracy for spinning spacecraft are widely discussed in Refs.1, 2. Specifically, the estimates of an attitude filter that relies on the dynamics propagation<sup>2,5,7</sup> are highly dependent on the accurate knowledge of the inertia tensor<sup>2</sup>. This also helps to improve the SAT. For earlier spin-stabilized spacecraft, the efforts were mostly focused on minimizing the tilt, which was typically sufficient to satisfy the mission requirements. Nevertheless, as more accurate attitude sensors became available the sensor-induced attitude estimation error diminished and the tilt became the dominant error source.

The system requirement allowance for spin-axis tilt may be in the range of tenths of a degree. For JAXA's ERG (Exploration of Energization and Radiation in Geospace) spacecraft the expected maximum value of the tilt angle is 1 deg and this value must be estimated with a least sum-of-squares accuracy of 0.1 deg<sup>5</sup>. The star scanner onboard ERG makes SAT estimation at this level of accuracy possible. Similarly, NASA's MMS (Magnetospheric Multiscale) mission spacecraft has star trackers, which are functional due to the slow spin rate of the spacecraft. Outputs of these sensors enable SAT estimation with an accuracy significantly better than the reference attitude accuracy of 0.1 deg<sup>2,8</sup>. Despite this evident requirement for SAT estimation for recent spinning spacecraft, the number of proposed estimation methods in the literature is very limited and they do not always possess practicability as they may be limited to specific sensors<sup>5</sup>.

In this paper, we evaluate a straightforward SAT estimation algorithm with the help of real data. The algorithm is based on the Singular Value Decomposition (SVD) and makes use of the attitude rates estimated by an attitude filter. It was previously presented and tested with simulated data for the ERG spacecraft, see Ref. 5. The simulation results show that the SVD algorithm for SAT estimation (SVD-SAT) can achieve SAT estimation at an accuracy level of tens of arcsec and is robust against other biases such as sensor misalignments. Moreover the algorithm's accuracy is better than that of a straightforward averaging method, which is in essence the same as the method in Ref.8.

This study applies the SVD-SAT algorithm to the in-flight sensor data<sup>9</sup> collected by NASA's CONTOUR spacecraft. CONTOUR was designed and operated by Johns Hopkins University Applied Physics Laboratory, Laurel, MD, USA. It was launched in July 2002 and injected into an elliptical Earth-phasing orbit that lasted about 6 weeks. During this period the spacecraft was stabilized at nominal spin rates of either 20 or 60 rpm and used a combined Sun-Earth sensor for the attitude measurements. Specifically, the Earth-sensor measurements<sup>9</sup> are generated by two infrared pencil-beams and are affected by unknown time-varying biases which affect the attitude estimation accuracy accordingly.

The CONTOUR flight data provide us with two valuable test opportunities. First, we may test our algorithm on a spacecraft with relatively minor expected SAT because of CONTOUR's compact rigid structure and the professional pre-launch balancing. Second, we may evaluate the robustness of our algorithm with respect to the sensor biases. As discussed in Ref.10, different approaches for processing the individual pencil-beam measurements to estimate the Earth aspect angle (EAA) produce different residuals over the data intervals. Therefore, we may investigate whether the SVD-SAT algorithm is capable of producing valid and consistent estimates during different data intervals and assess its performance in the presence of actual in-flight biases.

The second section presents the sensor measurement models for the spinning spacecraft. In the third section we discuss the attitude filter, whose rate estimates are used as inputs for the SVD-SAT method. Also in this section we discuss the effects of SAT on the spacecraft dynamics. In

the fourth section we present the SVD-SAT algorithm and evaluate its performances with the help of the real sensor data. The last section concludes the paper.

### SENSOR MEASUREMENT MODELS FOR SPINNING SPACECRAFT

A combined Earth-Sun sensor is used for attitude measurements onboard the CONTOUR spacecraft<sup>9</sup>. The measurement model for unit-vector measurements is simply,

$$\mathcal{S}_b = A_i^b \mathcal{S}_i + \mathbf{v} , \quad (1)$$

where,  $\mathcal{S}_b$  is the measurement vector in the body frame,  $\mathcal{S}_i$  is the reference vector in the inertial frame,  $A_i^b$  is the attitude matrix that transforms a vector from inertial to body frame and  $\mathbf{v}$  is the measurement noise. With reference to the geometry of the measurements (Fig.1) the unit vector measurements in the body frame can be formed as

$$\mathcal{S}_b^{sun} = \begin{bmatrix} \sin \nu \cos \delta \\ \sin \nu \sin \delta \\ \cos \nu \end{bmatrix} , \quad (2a)$$

$$\mathcal{S}_b^{earth} = \begin{bmatrix} \sin \beta \cos(\delta + \alpha) \\ \sin \beta \sin(\delta + \alpha) \\ \cos \beta \end{bmatrix} , \quad (2b)$$

using the sensor outputs for Sun-sensor and Earth-sensor measurements, respectively.

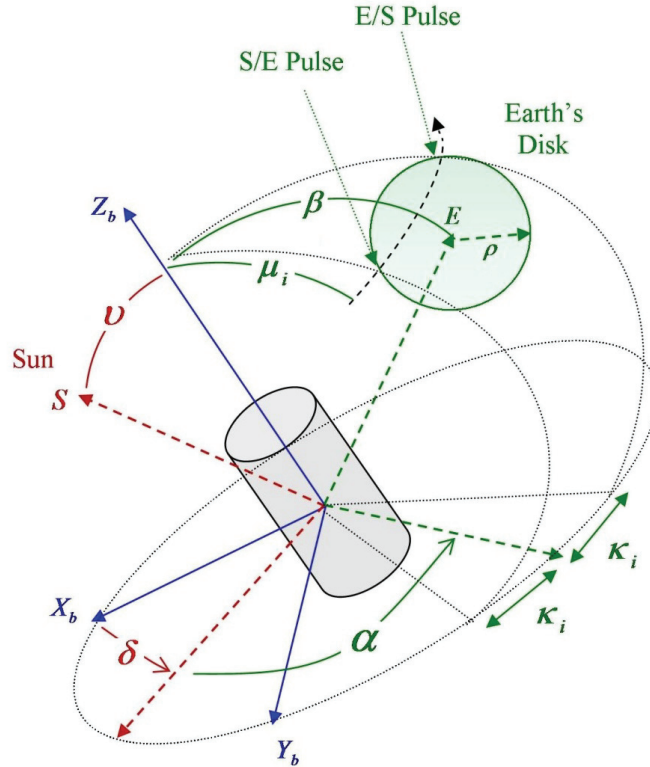


Figure 1. Geometry for Sun and Earth-sensor measurements.

The construction of the Sun-sensor unit-vector measurements is relatively easy. A typical V-slit Sun-sensor for a spinning satellite provides the Sun crossing times and the Sun aspect angle (SAA),  $\nu$ , which is the angle between the spin axis (i.e., body  $Z_b$  axis in Fig. 1) and the Sun direction  $\mathcal{S}$ . When considering the rotation angle shift of the Sun-sensor vertical slit plane relative to the body  $X_b$  axis, i.e. angle  $\delta$ , we can calculate the unit vector measurement at the time of Sun crossing as in Eq.(2a).

The Earth-sensor has two pencil-beams oriented at angles  $\mu_i$  ( $i=1, 2$ ) with respect to the spin axis. Each pencil-beam measures the crossing times for Space/Earth (S/E) and Earth/Space (E/S) infra-red boundaries. With the knowledge of the spin rate, these crossing pulses can be transformed into the half-chord angles  $\kappa_i$  ( $i=1, 2$ ), which are the fundamental measurements produced by the Earth-sensor. By using these measurements and as well the apparent Earth radius angle,  $\rho$ , we find the relationship for the EAA,  $\beta$ , from the spherical geometry (Fig.1):

$$\cos \mu_i \cos \beta + \sin \mu_i \cos \kappa_i \sin \beta = \cos \rho \quad i=1,2 \quad . \quad (3)$$

Here, the instantaneous value for the apparent Earth radius angle,  $\rho$ , can be calculated as  $\rho(t) = \sin^{-1}(R_{IR} / r(t))$ , where  $r$  is the orbital radius and  $R_{IR}$  is the Infrared (IR) Earth radius. Note that the nominal value of  $R_{IR}$  is  $\sim 40\text{km}$  above the Earth radius<sup>11</sup>. The actual value of  $R_{IR}$  is unknown and varies over time and location.

In fact, the scan paths of each of the two IR pencil-beams over the Earth are different due to different mounting angles ( $\mu_1$  and  $\mu_2$ ). As a result, their S/E and E/S crossings are at *different* locations on the Earth's IR rim. Therefore, the two  $\rho$  values observed by the IR sensors will in general differ under seasonal, diurnal, and local variations in the IR radiation intensities. This is the main reason why the two individual pencil-beams produce different biases  $\Delta\rho_i = \rho - \rho_{p,i}$  (where  $\rho_{p,i}$  are the predicted values) that have been reconstructed by using the estimated attitude as shown in Fig.10 of Ref.10. Yet it is very hard to model all of these effects realistically so we assume, a priori, that the Earth's IR radius is perfectly uniform so we may use the same  $\rho$  value for both IR beams.

We may use different methods to derive the EAA when there are two individual pencil-beams. To start with, we may rewrite the Eq.(3) in the form<sup>10</sup>:

$$b_i \cos \chi_i \cos \beta + b_i \sin \chi_i \sin \beta = \cos \rho \quad i=1,2 \quad , \quad (4)$$

where the auxiliary functions are defined as:

$$b_i = \sqrt{1 - (\sin \mu_i \sin \kappa_i)^2} ; \quad \chi_i = \arctan(\tan \mu_i \cos \kappa_i) \quad i=1,2 \quad (5a,b)$$

Thus, each pencil-beam gives its own EAA solution,  $\beta_i$  :

$$\beta_i^\pm = \chi_i \pm \arccos\{\cos(\rho) / b_i\} \quad i=1,2 \quad (6)$$

One method to construct a single EAA value to use in the estimator is to take the average of the two different  $\beta_i$  values produced by each of the two pencil-beams as  $\beta_{ave} = (\beta_1^\pm + \beta_2^\pm) / 2$ , after the sign ambiguity is resolved. The second method is to calculate an optimal (in a minimum variance sense)  $\beta_{opt}$  value as a weighted combination of the two individual  $\beta_i$  angles. This

method is based on the sensitivity analysis for each of the two  $\beta_i$  solutions with respect to the half-chord angle measurements,  $\kappa_i$ . For brevity we do not present further details of the analysis and refer the reader to Ref. 10.

Lastly, a single solution for  $\beta$  may be calculated from the two distinct relationship equations (Eq.3) for the two pencil beams without requiring the individual  $\beta_i$  solutions (Eqs.4-6). Since we assume here that the  $\rho$  value is identical for both pencil-beam scans we obtain the single  $\beta_{sin}$  solution as,

$$\beta_{sin} = \arctan\left(\frac{\cos \mu_1 - \cos \mu_2}{\sin \mu_2 \cos \kappa_2 - \sin \mu_1 \cos \kappa_1}\right). \quad (7)$$

In this study, we use two individual solutions for  $\beta$ , which are the “optimal beta”  $\beta_{opt}$  and the “single beta”  $\beta_{sin}$  of Eq. (7) to build two different sets of unit-vector measurements from the Earth-sensor outputs. Having two different  $\beta$  values gives us the opportunity to compare the results, especially for the SAT estimation, as these two values contain different unknown biases.

Fig. 2 gives the derived EAAs from the chord measurements and includes  $\beta_1$  and  $\beta_2$  values for each pencil-beam, which are calculated with Eqs.(5,6). The usable good data, which is least corrupted by sensor biases, is collected during the scans over Earth’s mid-latitude region that starts approximately at 36.6h since the perigee pass and lasts for about 1h<sup>10</sup>. The interval before the mid-latitude region should be avoided because it is near the singularity in the chord-length measurements for the second pencil-beam and the same should be done for the first pencil-beam after the mid-latitude region.

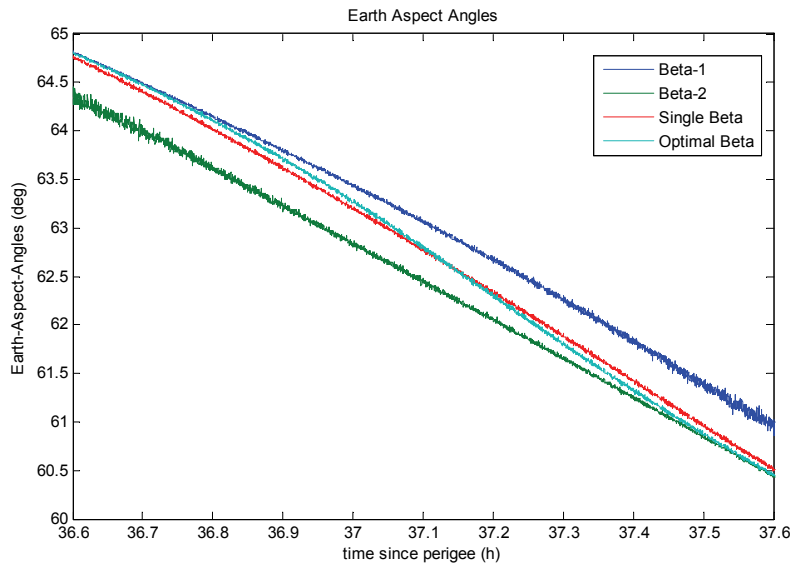


**Figure 2. Earth aspect angles derived from chord measurements.**

Fig. 3 presents the residuals that each EAA produces within the mid-latitude region. It is simply the difference between the derived EAA measurements shown in Fig.2 and the  $\beta_p$  value which is predicted by using the attitude estimate obtained with the recursive SpinUKF filter, whose de-

tails will be introduced in the next section. The  $\beta_{opt}$  solution gradually shifts from  $\beta_1$ , which has the lower variance at the beginning of the interval, to  $\beta_2$ , which has the lower variance at the end. On the other hand,  $\beta_{sin}$  has smaller and almost constant residuals throughout the interval. Surely one of the advantages of using  $\beta_{sin}$  is not requiring any  $\rho$  angle information when calculating the EAA. Although it may appear that biases in the local IR Earth-radii have been avoided, the IR biases still affect the calculated  $\beta_{sin}$  values through their propagation into the  $\kappa_i$  measurements. Thus the advantages we have for not using  $\rho$  angle information for  $\beta_{sin}$  calculation is limited.

Although  $\beta_{sin}$  has smaller residuals compared to  $\beta_{opt}$ , both solutions have similar variances over the mid-latitude region:  $\sigma_{\beta_{sin}}^2 = 1.5325 \times 10^{-4} \text{ deg}^2$  and  $\sigma_{\beta_{opt}}^2 = 1.4625 \times 10^{-4} \text{ deg}^2$ .

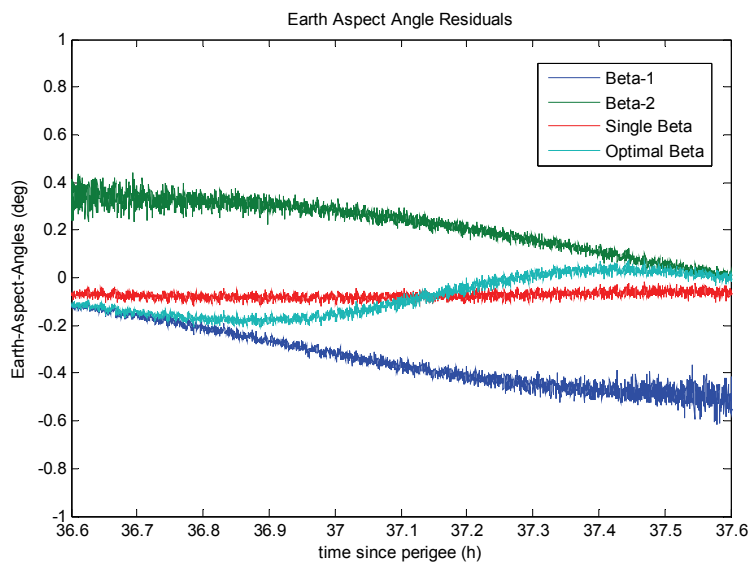


**Figure 3. Residuals of the Earth aspect angle in the mid-latitude region.**

To build the unit-vector measurements for the Earth-sensor (Eq.2b) the Sun-Earth dihedral angle,  $\alpha$ , is also needed. Calculation of this angle from two distinct  $\alpha_i$  measurements of the pencil-beams is straightforward as these two measurements can be equally weighted as,

$$\alpha = (\alpha_1 + \alpha_2) / 2. \quad (8)$$

## ATTITUDE FILTER

### Filtering Algorithm

The SVD-SAT algorithm requires attitude rate knowledge in the spacecraft body frame during the period in which the SAT bias is investigated. The spinning spacecraft usually do not carry gyros onboard. Thus, an estimator which propagates the Euler dynamical equations and estimates the attitude rate of the spacecraft together with the attitude angles must be used.

Different filtering algorithms have been proposed for spin-stabilized spacecraft that are capable of estimating the attitude rate in the body frame<sup>7,12,13</sup>. In this study we prefer using the

SpinUKF<sup>13</sup> as the filtering algorithm. The SpinUKF is essentially an UKF with the following state components: the spin-axis unit-vector direction terms  $(x, y, z)$  in the inertial frame, the spin-phase angle  $\gamma$ , and the body angular rate vector  $\boldsymbol{\omega}$  with respect to the inertial frame,

$$\mathbf{X} = [x \quad y \quad z \quad \gamma \quad \boldsymbol{\omega}]^T. \quad (9)$$

The UKF is derived for discrete-time nonlinear equations, so the system model is given by:

$$\mathbf{X}_{k+1} = \mathbf{f}(\mathbf{X}_k, k) + \mathbf{w}_k, \quad (10a)$$

$$\mathbf{Y}_k = \mathbf{h}(\mathbf{X}_k, k) + \mathbf{v}_k. \quad (10b)$$

Here,  $\mathbf{X}_k$  is the state vector and  $\mathbf{Y}_k$  is the measurement vector at time  $t_k$ . Moreover,  $\mathbf{w}_k$  and  $\mathbf{v}_k$  are the process and measurement error noises, which are assumed to be Gaussian white noise processes with covariance matrices  $\mathbf{Q}(k)$  and  $\mathbf{R}(k)$ , respectively. We estimate the inertial attitude of the spacecraft while the process is propagated by using the discrete-time versions of,

$$\dot{x} = \left( \frac{xzs(\gamma) + yc(\gamma)}{r} \right) \omega_x + \left( \frac{xzc(\gamma) - ys(\gamma)}{r} \right) \omega_y, \quad (11a)$$

$$\dot{y} = \left( \frac{yzs(\gamma) - xc(\gamma)}{r} \right) \omega_x + \left( \frac{yzc(\gamma) + xs(\gamma)}{r} \right) \omega_y, \quad (11b)$$

$$\dot{z} = -rs(\gamma)\omega_x - rc(\gamma)\omega_y, \quad (11c)$$

$$\dot{\gamma} = \omega_z - \frac{z}{r} (s(\gamma)\omega_y + c(\gamma)\omega_x), \quad (11d)$$

and the Euler's dynamics equation which is required in the absence of gyros,

$$\dot{\boldsymbol{\omega}} = \mathbf{J}^{-1} [\mathbf{N} - \boldsymbol{\omega} \times (\mathbf{J}\boldsymbol{\omega})]. \quad (12)$$

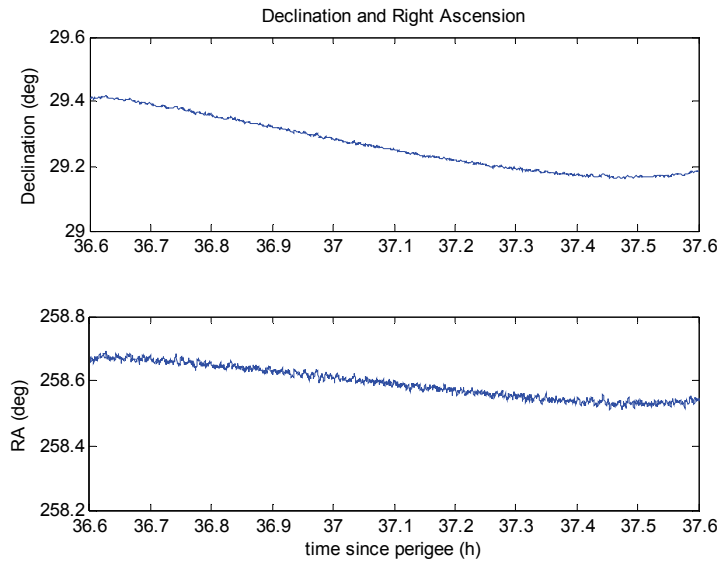
Here  $c(\cdot)$  and  $s(\cdot)$  are  $\cos(\cdot)$  and  $\sin(\cdot)$  functions, respectively,  $r = \sqrt{x^2 + y^2}$ ,  $\mathbf{J}$  is the inertia matrix of the spacecraft and  $\mathbf{N}$  is the torque vector, which is sum of the external disturbance torques such as solar radiation pressure and control torques, if there are any. We shall note that, in this study, values of the external disturbance torque are not provided to the filter and there is no actuator input for the specific period, so  $\mathbf{N}$  is a zero vector. For a detailed introduction and analyses of the SpinUKF the reader may refer to Ref.13.

Fig. 4 gives the evolution of the estimated attitude produced by SpinUKF for CONTOUR during the mid-latitude interval in terms of the right ascension (RA) and declination (DE) angles. The mean of these values is

$$\text{RA} = 258.594^\circ; \quad \text{DE} = 29.265^\circ, \quad (13)$$

which is  $0.066^\circ$  in arc-length distance away from the values estimated with the Tanygin-Shuster algorithm in Ref. 10. Note that the  $\beta_{sin}$  values for the EAA have been used in these results.

Fig.5 gives the estimated transverse angular velocities in the body frame produced by SpinUKF. The red line denotes the "0 deg/s". The SVD-SAT algorithm uses these rate values to estimate the SAT angle.



**Fig. 4. RA and DE attitude angles estimated with the SpinUKF.**

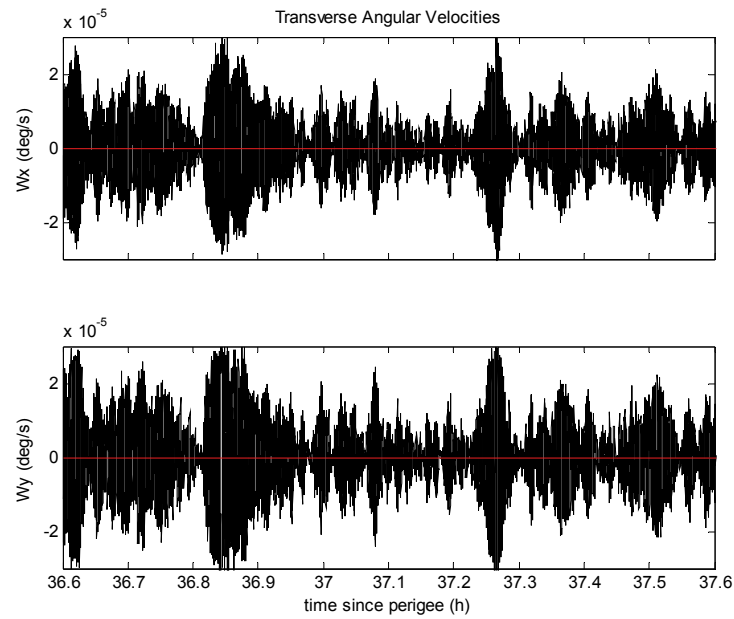


**Fig. 5. Transverse angular velocities estimated with the SpinUKF.**

### Effects of Spin-Axis Tilt on Attitude Filter Estimates

The tilt error is observed as the mismatch between the actual spin axis that corresponds to the maximum (or minimum) principal axis of inertia, i.e. the principal  $Z$  axis (or  $-Z_p$ ) and the body  $Z$  axis (or  $-Z_b$ ), see Fig. 6, which is the intended spin axis during the design phase. The SAT can be



represented as a rotation between the principal and body frames of the spacecraft and is described by the small Tait-Bryan angles,  $\theta_{cx}$  and  $\theta_{cy}$ . Assuming the rotation angles are small, the rotation matrix that transforms from the principal frame to the body frame is<sup>5</sup>,

$$C_{bp} = \begin{bmatrix} 1 & 0 & \theta_{cy} \\ 0 & 1 & -\theta_{cx} \\ -\theta_{cy} & \theta_{cx} & 1 \end{bmatrix}. \quad (14)$$

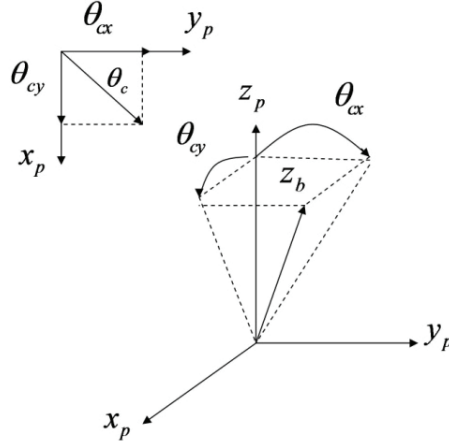


**Fig.6. Spin-axis tilt (SAT).**

In case of SAT the spacecraft's moments of inertia in the body frame differ from its inertia moments in the principal frame. The relation between these two inertia characteristics can be shown as

$$J_b = C_{bp} J_p C_{bp}^T, \quad (15)$$

where,  $J_b$  is the inertia matrix in the body frame and  $J_p$  is the spacecraft's inertia matrix in the principal frame. The effects of the SAT are observed in the estimation of the spin-axis terms in the inertial frame in two forms: Systematic bias (non-zero mean attitude residuals) and deviations around the mean (covariance increase)<sup>5</sup>.

Any SAT error also affects the body rate estimates. Assuming there is no nutation, the spacecraft attitude rate vector in the principal frame may be given as,

$$\boldsymbol{\omega}_p = [0 \quad 0 \quad \omega_z]^T. \quad (16)$$

Then the attitude rate observed in the body frame becomes,

$$\boldsymbol{\omega}_b = C_{bp} \boldsymbol{\omega}_p = [\theta_{cy} \omega_z \quad -\theta_{cx} \omega_z \quad \omega_z]^T. \quad (17)$$

Clearly there is a shift (bias) in the mean of attitude rates and this shift is proportional to the coning angle times the spin rate. The exact phenomenon has been observed for the MMS spacecraft (see Fig.5 of Ref.2).

For the CONTOUR spacecraft Fig.5 shows that there is no bias in the estimated transverse angular rates. Thus, we conclude that the spin-axis tilt for the spacecraft (at least during the period of observation) is negligible and the SVD-SAT algorithm should produce results in accordance.

## SPIN-AXIS TILT ESTIMATION

### The SVD-SAT Algorithm

The objective of the SVD-SAT algorithm is finding the rotation matrix which transforms the angular velocity vector in the body frame (estimated by the attitude filter) to the angular velocity vector in the principal frame. The spin rate around the major principal axis is measured by the Sun-sensor using the time log for consecutive Sun crossings.

The cost function that is to be minimized using the SVD-SAT is

$$L(\theta_{cx}, \theta_{cy}) = \frac{1}{2} \sum_l a_l \left| \boldsymbol{\omega}_p^l - \hat{C}_{pb}(\theta_{cx}, \theta_{cy}) \hat{\boldsymbol{\omega}}_b^l \right|^2. \quad (18)$$

Here the hat operator denotes the estimated quantities,  $a_l$  is the sampling weight,  $\hat{\boldsymbol{\omega}}_b^l = [\hat{\omega}_{bx}^l \ \hat{\omega}_{by}^l \ \hat{\omega}_{bz}^l]$  is the angular velocity vector in the body frame which is estimated by the SpinUKF filter and  $\boldsymbol{\omega}_p^l$  is the angular velocity vector in the principal frame for the  $l^{\text{th}}$  measurement.  $\boldsymbol{\omega}_p^l$  is given as,

$$\boldsymbol{\omega}_p^l = [0 \ 0 \ \tilde{\omega}_{pz}^l]^T. \quad (19)$$

$\tilde{\omega}_{pz}^l$  is the spin rate measured by the Sun-sensor,

$$\tilde{\omega}_{pz}^l = \frac{2\pi}{t_{k+1} - t_k} + \nu_t, \quad (20)$$

and corrupted with zero-mean white noise  $\nu_t$  that depends on the Sun-sensor timing error. Since we use only the Sun-sensor measurements, all the samples are equally weighted, i.e.  $a_l = 1$  for  $l = 1 \dots n$  in Eq.(18). To avoid misunderstanding we shall note that we assume that there is no nutation for the spacecraft. Actually, the CONTOUR Sun-sensor measurements show that nutation is negligible throughout the interval considered here.

The cost function (18) is minimized using the SVD method. The main advantage of the SVD over other algorithms is that it provides numerically robust solutions. The SVD method is well known<sup>14</sup> but we present it here for completeness. We can write Eq. (18) in a more convenient form as,

$$L(\hat{C}_{bp}) = \Gamma_0 - \text{tr}(\hat{C}_{pb} \Omega^T), \quad (21)$$

where,

$$\Gamma_0 = \sum a_l, \quad (22a)$$

$$\Omega = \sum a_l \boldsymbol{\omega}_p^l (\hat{\boldsymbol{\omega}}_b^l)^T. \quad (22b)$$

Hence, the cost function minimization problem reduces into the problem of maximizing the trace,  $\text{tr}(\hat{C}_{pb} \Omega^T)$ . There are many single frame methods for solving this problem. The SVD is one of the most accurate, reliable and robust methods amongst them. The matrix  $\Omega$  has the singular value decomposition:

$$\Omega = U \Sigma^T V^T = U \text{diag}[\Sigma_{11} \ \Sigma_{22} \ \Sigma_{33}] V^T, \quad (23)$$

where  $U$  and  $V$  are orthogonal and the singular values obey  $\Sigma_{11} \geq \Sigma_{22} \geq \Sigma_{33} \geq 0$ . Then we can show that the trace is maximized and the optimal transformation matrix can be obtained as

$$U^T \hat{C}_{pb}^{opt} V = \text{diag}[1 \quad 1 \quad \det(U)\det(V)], \quad (24a)$$

$$\hat{C}_{pb}^{opt} = U \text{diag}[1 \quad 1 \quad \det(U)\det(V)] V^T. \quad (24b)$$

Note that the estimated transformation matrix  $\hat{C}_{pb}^{opt}$  corresponds to the estimate for the transpose of the rotation matrix given in Eq.14. The estimation accuracy can be evaluated by examining the covariance matrix for the rotation angle error. If the secondary singular variables are defined as,  $s_1 = \Sigma_{11}$ ,  $s_2 = \Sigma_{22}$ ,  $s_3 = \det(U)\det(V)\Sigma_{33}$  then the covariance matrix  $P_{svd}$  is calculated as,

$$P_{svd} = U \text{diag}[(s_2 + s_3)^{-1} \quad (s_3 + s_1)^{-1} \quad (s_1 + s_2)^{-1}] U^T. \quad (25)$$

### The Averaging Algorithm

The averaging method is a straightforward approach that is based on the method given in Ref.8. Our approach differs from the one applied to the MMS spacecraft because we prefer a direct calculation for the SAT angles by averaging the terms of the angular-momentum vector in the body frame. In Ref.8 a fully populated direction cosine matrix is calculated instead. The steps for our averaging algorithm are,

- Time-average  $\hat{\mathbf{i}}_i^{spin} = [x \quad y \quad z]^T$  terms to obtain the angular momentum vector in the inertial frame. The resulting vector is  $\hat{\mathbf{i}}_i^{ang}$  and this is the vector around which the  $Z_b$  axis rotates in inertial space. Here, the underscore indicates the time-averaged vector.
- Transform this angular momentum vector in inertial frame to the body frame using the estimated attitude history as

$$\hat{\mathbf{i}}_b^{ang}(t) = A(t) \hat{\mathbf{i}}_i^{ang} \quad t = t_o \dots t_{end}. \quad (26)$$

Here,  $A(t)$  is the attitude matrix of the spacecraft at  $t$  in terms of the spin-axis unit-vector direction terms  $(x, y, z)$  in the inertial frame and the spin-phase angle  $\gamma$ .

- Time-average the first two terms of  $\hat{\mathbf{i}}_b^{ang}$  vector, which are coinciding to the angular momentum in  $X_b$  and  $Y_b$  axes. In case there is no tilt  $\hat{\mathbf{i}}_{bx}^{ang}$  and  $\hat{\mathbf{i}}_{by}^{ang}$  must vanish, which means the angular momentum vector in the body frame matches with the  $Z_b$  axis. On contrary, if there is a tilt, the averaged values give the Tait-Bryan angles in radians when assuming that these angles are small.

### Performance Evaluation with Real Data

Using the attitude rate estimates over the mid-latitude region (in between 36.6h and 37.6h from the perigee pass in Fig.5), the SVD-SAT algorithm estimates the tilt angles as,

$$\theta_{cx} = -4.087 \times 10^{-10} \text{ deg}; \quad \theta_{cy} = 3.8581 \times 10^{-10} \text{ deg}. \quad (27)$$

As expected from the transverse angular velocities in the body frame (Fig. 5) the SAT error is negligible for CONTOUR, at least during the interval considered.

The graphical representation for the estimated tilt angles by the averaging method is given in Fig.7. Terms of angular momentum vector in body X and Y axes are plotted for the complete attitude history. Time-averaged values, which indicate the estimated tilt angles, are indicated with the red dot. As noted on the Figure, the estimated values are,

$$\theta_{cx} = -2.3242 \times 10^{-5} \text{ deg}; \quad \theta_{cy} = -1.1767 \times 10^{-5} \text{ deg}. \quad (28)$$

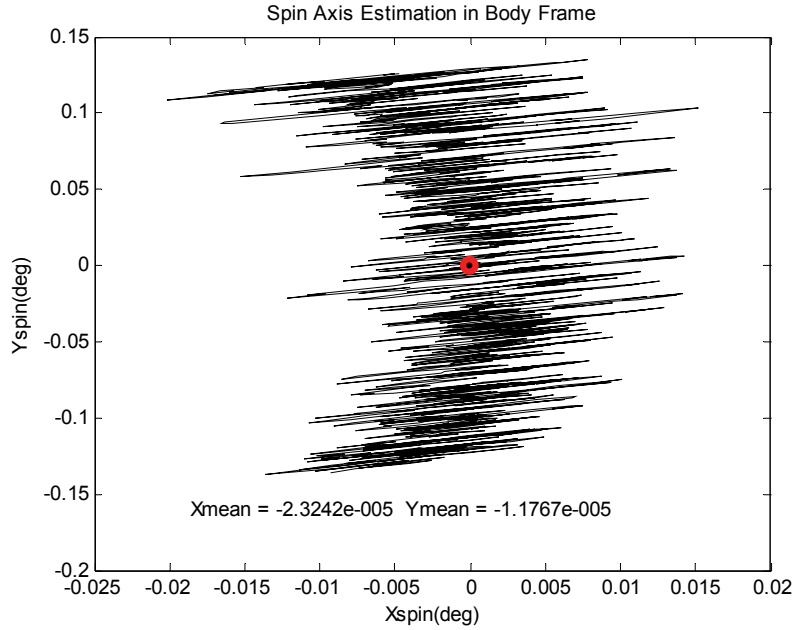


**Fig. 7. Spin axis tilt estimation by the averaging method for the 36.6h – 37.6h interval.**

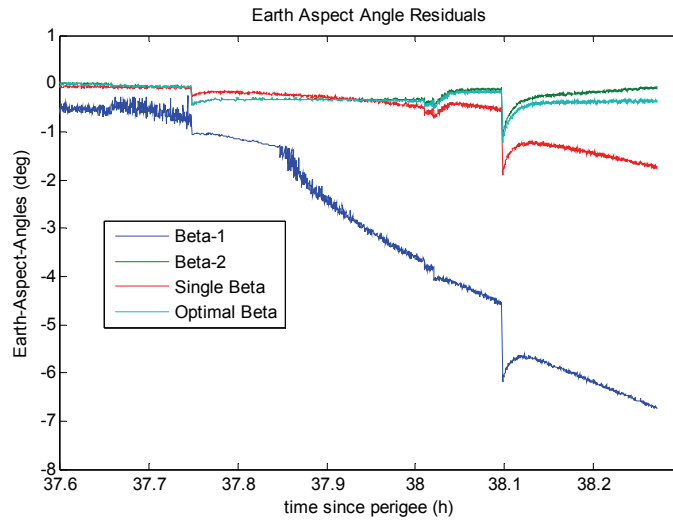
The results for the averaging method are also at a negligible level, yet roughly  $5 \times 10^4$  times higher than those of the SVD-SAT method. The main reason is the lower accuracy of the averaging method; the estimation error occasionally exceeds a few arcmins<sup>5</sup>.

Next, the accuracy of the SVD-SAT algorithm is investigated when there are severe biases in the measurements. For the Earth-sensor we know that the measurements of the first pencil-beam deteriorate after 37.6h from the perigee pass because of sensor performance degradations for short Earth-scan intervals. Furthermore, the measurement sensitivity decreases and the IR biases increase. In fact, this data should not be used for attitude-estimation purposes since the sensor has been designed and calibrated to ensure specified performances over the Earth’s mid-latitude region only.

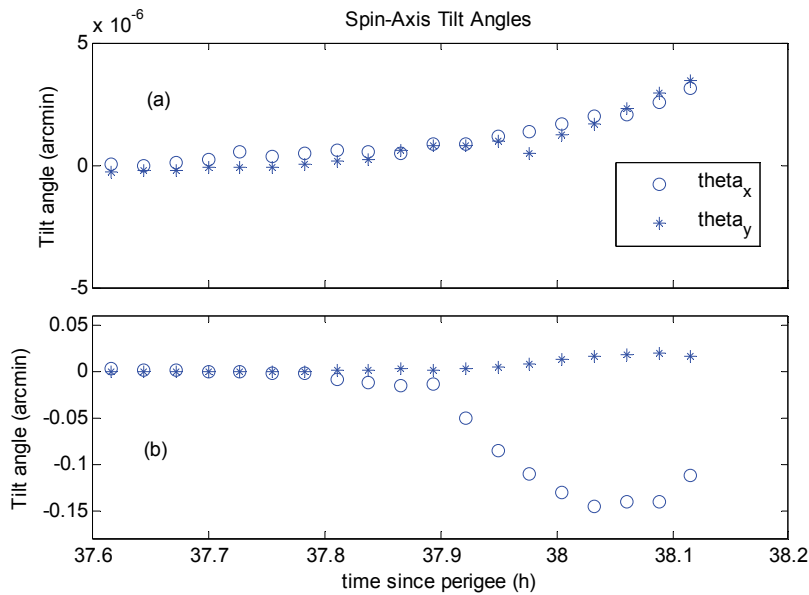
Our purpose here aims at testing the SAT estimation algorithms in a situation where the measurements are severely contaminated by biases. Fig.8 shows clearly how the EAA residuals for the first pencil-beam increase during this period. As a result, also the “optimal-beta” and “single-beta” solutions used in the attitude filter diverge rapidly. As expected, also in this situation, the optimal-beta solution shows better residuals than the single-beta solution.

Fig.9 shows the SAT estimation results for both the SVD-SAT and averaging algorithms. Estimations are performed within a sliding window for a window size of 1000s and, at every calculation, the starting time of the estimation window is advanced by 100s. Results for each estimation window are given at its mid-point time.  $\beta_{sin}$  is used as the EAA for the measurements in the SpinUKF. Apparently, as the bias in the measurements increases, the bias in the SAT estimations of both the SVD-SAT and averaging algorithms also increases. Yet this increase in the SVD-SAT algorithm’s estimations is at a negligible level compared to those of the averaging method (note the different scales for the two algorithms). The bias in the estimates of the averaging method

becomes as large as 0.15 arcmin and follows the trend in the Earth-sensor measurements over time (of course with a delay and attenuation as the estimations are performed within a window).



**Figure 8. Residuals of the Earth aspect angle when the measurements are biased.**



**Fig. 9. Spin axis tilt estimation when the measurements are biased. “Single beta” is used as the EAA measurements in the SpinUKF.**  
**a) Results of SVD-SAT method; b) Results of Averaging method.**

If we use  $\beta_{opt}$  as the EAA for the measurements in the SpinUKF, the bias in the SAT estimation reduces (Fig.10) as the bias in the measurements also decreases (Fig.8). The maximum bias in the averaging method estimations is now 0.1 arcmin. The results confirm that the averaging method is more sensitive to the measurement biases whereas the SVD-SAT algorithm is more robust. In this sense the performance evaluation with real data supports the results we obtained with the numerical simulations in Ref.5. Since we use the SpinUKF attitude rate estimates for

spin-axis tilt estimation, the accuracy of the SVD-SAT does not vary significantly in the presence of measurement biases. The algorithm is capable to accurately estimate the tilt angle independently from the magnitude of the bias. The robustness of the SVD algorithm is another reason for its insensitivity to the other errors.

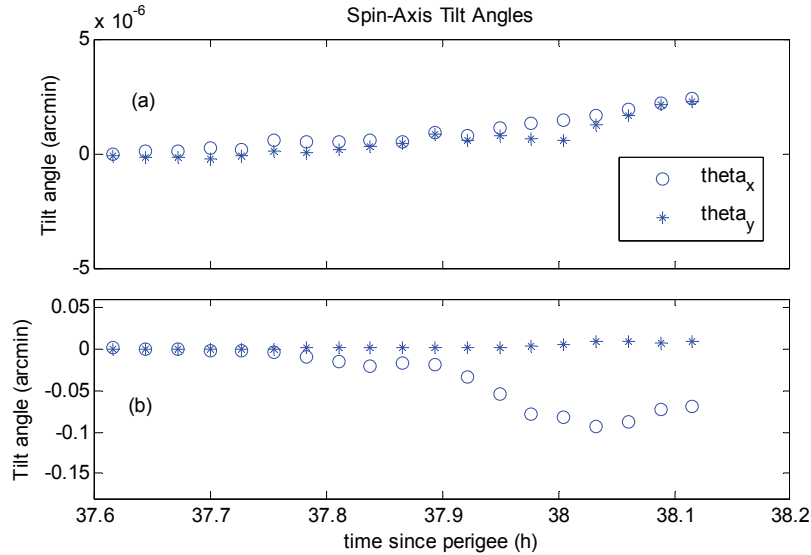


**Fig. 10. Spin axis tilt estimation when the measurements are biased. “Optimal beta” is used as the EAA measurements in the SpinUKF.**  
**a) Results of SVD-SAT method; b) Results of Averaging method.**

## CONCLUSION

A straightforward algorithm for spin-axis tilt (SAT) estimation is evaluated with the help of in-flight data collected by the spinning spacecraft CONTOUR. The algorithm is based on the Singular Value Decomposition (SVD) and makes use of the attitude rates estimated by the SpinUKF attitude filter. The results show that the spacecraft’s SAT error is negligible in the specific interval where the operational attitude measurement data is gathered. Further investigations based on non-nominal biased Earth-sensor measurements confirm that the algorithm is able to produce robust attitude estimates that are not significantly affected by the other biases.

## ACKNOWLEDGMENTS

The authors appreciate the help of Dr. Wayne Dellinger of Applied Physics Laboratory, Laurel, MD, USA, in facilitating the use of CONTOUR’s in-flight sensor data in the present paper.

This research is supported in part by the ERG project of ISAS/JAXA.

## REFERENCES

- <sup>1</sup> J.C. Van der Ha, “Spin Axis Attitude Determination Accuracy Model in the Presence of Biases,” *Journal of Guidance, Control, and Dynamics*, Vol.29, No.4, 2006, pp.799-809.
- <sup>2</sup> J.C. Raymond, J.E. Sedlak and B. Vint, “Attitude Ground System (AGS) for the Magnetospheric Multiscale (MMS) Mission,” *Proceedings 25<sup>th</sup> International Symposium on Space Flight Dynamics*, Munich, Germany, 2015.

- <sup>3</sup> J.R. Wertz (ed.), *Spacecraft Attitude Determination and Control*, Kluwer Academic Publishers, Dordrecht, Holland, 1978, p. 489.
- <sup>4</sup> L. Fraiture, "Spin-Axis Attitude Estimation by a Controlled Correlation Method," *Journal of Spacecraft and Rockets*, Vol.42, No.1, 2005, pp. 58-65.
- <sup>5</sup> H.E. Soken, S. Sakai, K. Asamura, Y. Nakamura and T. Takashima, "Spin-Axis Tilt Estimation for Spinning Spacecraft," *Proceedings AIAA Guidance, Navigation and Control Conference*, AIAA 2016-0626, San Diego, USA, 2016.
- <sup>6</sup> U.J. Shankar, M.N. Kirk and G.D. Rogers, "Van Allen Probes On-Orbit Verification of Spacecraft Dynamics," *Proceedings 24<sup>th</sup> International Symposium on Space Flight Dynamics*, Maryland, USA, 2014.
- <sup>7</sup> R.R. Harman, "An Empirical Comparison Between Two Recursive Filters for Attitude and Rate Estimation of Spinning Spacecraft," *Proceedings AIAA/AAS Astrodynamics Specialist Conference and Exhibit*, AIAA 2006-6158, Colorado, USA, 2006.
- <sup>8</sup> J.E.Sedlak, E.A. Superfin, and J.C. Raymond, "Magnetospheric Multiscale (MMS) Mission Attitude Ground Segment Design," *Proceedings 22nd International Symposium on Space Flight Dynamics*, Sao Jose dos Campos, Brazil, 2011.
- <sup>9</sup> J.C. Van der Ha, G. Rogers, W. Dellinger, and J. Stratton, "CONTOUR Phasing Orbits: Attitude Determination & Control Concepts & Flight Results," *Advances in the Astronautical Sciences*, Vol. 114, Part II, 2003, pp. 767-781.
- <sup>10</sup> J.C. Van der Ha, "Spin Axis Attitude Determination Using In-Flight Data," *Journal of Guidance, Control, and Dynamics*, Vol.33, No.3, 2010, pp.768-780.
- <sup>11</sup> M.J. Sidi, *Spacecraft Dynamics & Control - A Practical Engineering Approach*, Cambridge University Press, UK, 1997, p.337.
- <sup>12</sup> F.L. Markley and J.E. Sedlak, "Kalman Filter for Spinning Spacecraft Attitude Estimation," *Journal of Guidance, Control, and Dynamics*, Vol. 31, No.6, 2008, pp.1750-1760.
- <sup>13</sup> H.E. Soken, S. Sakai, K. Asamura, Y. Nakamura and T. Takashima "Spin Parameters and Nonlinear Kalman Filtering for Spinning Spacecraft Attitude Estimation," *Proceedings 27<sup>th</sup> AAS/AIAA Space Flight Mechanics Meeting*, AAS 17-249, San Antonio, TX, USA, 2017.
- <sup>14</sup> F.L. Markley and J.L. Crassidis, *Fundamentals of Spacecraft Attitude Determination and Control*, Springer, New York, USA, 2014, pp.196-197.